MODELLING THE DAMAGE EVOLUTION IN UNIDIRECTIONAL ALL-CARBON HYBRID LAMINATES

Amaury, Ollic[a], Fariborz, Sheibanian[b], Babak, Fazlali[c], Yentl, Swolfs[c], Stepan V., Lomov[c], Valter, Carvelli[a]

a: Department A.B.C., Politecnico di Milano, Milan, Italy – amaury.ollic@gmail.com
b: Department of Aerospace Engineering, Amirkabir Univ of Technology, Tehran, Iran
c: Department of Materials Engineering, KU Leuven, Leuven, Belgium

Abstract: *A finite element model was developed to simulate the damage evolution in unidirectional (UD) all-carbon hybrid composites subjected to tensile loading. The finite element model exploits translaminar embedded cohesive elements governed by a unimodal Weibull strength distribution in the Low-Strain (LS) plies to simulate fragmentation. Interlaminar cohesive elements simulate the Low-Strain (LS) and High-Strain (HS) plies interfaces. The numerical analyses highlighted the evolution of the tensile behavior from pseudo-ductile to catastrophic delamination by changing the LS/HS thickness ratio. The distribution of translaminar strength of the LS material and the number of cracks simulated have a key role in the numerical mechanical response. The model had good agreement to experimental data for tensile behavior of thin-ply all-carbon hybrid laminates.*

Keywords: all-carbon hybrid laminates; pseudo-ductility; numerical model; damage evolution

1. Introduction

The lack of ductility of fiber reinforced composite materials can be overcome by interlayer hybridization where Low Strain (LS) material is sandwiched between High Strain (HS) material. Hybridization tends to improve composite properties but induces complex failure mechanisms, including multiple interacting damage modes, such as ply fragmentation and delamination [1]. Therefore, modelling the damage evolution of hybrid composites is more complex than that of non-hybrid composites. Few mechanical numerical models of fiber hybrid composites are available in the literature, to the authors' knowledge, and they are mainly dedicated to unidirectional reinforcements (see e.g. [2–4]).

Intrayarn random fiber packings have been considered to build three-dimensional finite element models in [3]. The models simulated the effect of the hybridization on the stress concentration around a broken carbon fiber. Modelling UD interlayer carbon/glass hybrid laminates has been detailed in [4], which concluded that one of the most important parameters influencing the damage is the ratio of LS thickness and the overall laminate thickness. The variation of this ratio allows to depict a damage mode map and to predict the failure behavior of new hybrid fiber reinforced composite configurations.

In this context, the present study was dedicated to the development of a finite element model to predict the tensile response of unidirectional all-carbon hybrid laminates. The numerical results were compared to experimental data available in [5].

2. Finite element modelling approach for tensile loading of UD hybrid laminates

The model considers an interlayer hybrid laminate configuration made of one layer of LS material and two layers of HS material. 3D cohesive elements are used at the LS/HS interface to simulate delamination. Fragmentation is simulated by cohesive elements embedded between two bulk elements of the LS layer, which properties are not affected [4]. The thickness of the cohesive elements is set to 0.3 µm. In real tensile tests, multiple fragmentation density and distribution may affect the damage evolution. However, in this work, a uniform distribution of possible fragmentation is supposed considering 319 cohesive elements along the specimen length (X), and, consequently, the length of the LS bulk element is 0.25 mm, which lead to a length of the specimen $l = 80$ mm. As discussed in [4], the distribution of cohesive elements alongside the length could cause unrealistic material softening behavior. To prevent it, a large penalty stiffness ($K = 10^9\ MPa/mm$) and a low viscosity parameter ($\mu = 10^{-6}\ Pa\ \cdot s$) have been used. Hence, the dimensions of the interface cohesive elements are 0.25 mm x 0.25 mm and thickness 0.3 µm, which is coherent with the suggestions in [6]. To simplify the approach, the stiffness and the fracture energy are assumed the same for all embedded cohesive elements. The random nature distribution of the fiber strength is represented by Weibull distribution.

The model geometry and boundary conditions represent a unidirectional tensile test. The model constraints are summarized in Figure 1, where U_X, U_Y and U_Z are the displacement component along X, Y and Z direction, respectively. To reduce the computation cost, symmetry was applied along the length and the thickness.

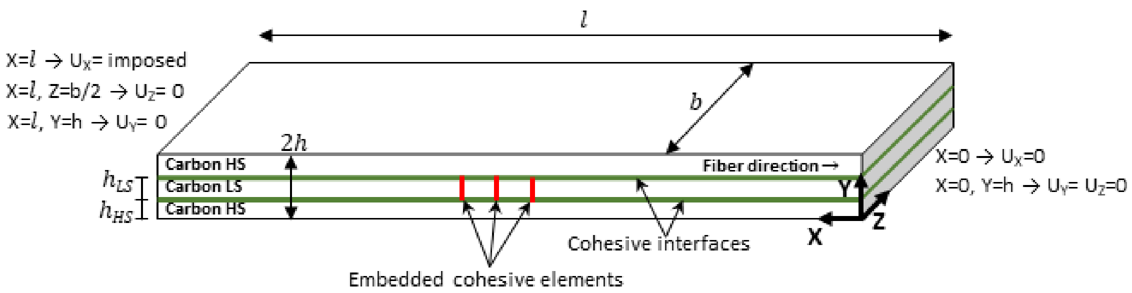

Figure 1. Sketch of the geometry, boundary conditions and multi-fragmentation of the all-carbon hybrid laminate3D model.

The length of the bulk element, namely the distance between two embedded cohesive elements, is 0.25 mm, which is lower than the recovery length of the LS layer. When failure occurs at a cohesive element position, the stress in nearby LS elements decreases. Hence, damage in some cohesive elements located within the recovery length is not activated due to the low stress level [7].

3. Numerical predictions of UD thin-ply all-carbon hybrid laminate

A UD thin-ply all-carbon hybrid laminate was experimentally investigated in [5]. It was produced with T1000 (T) carbon fibers for the high-strain (HS) layer (cured ply thickness 0.032 mm), and M55 (M) carbon fibers for the low-strain (LS) layer (cured ply thickness 0.031 mm). It had stacking sequence [T_2/M/T_2]. The geometry (with symmetries) and materials properties considered for the model of the thin-ply all-carbon hybrid laminate under tensile loading are listed in Table 1 [5].

Table 1: Features of the UD all-carbon thin-ply hybrid laminate finite element model.

Mechanical properties of HS and LS layers

	E_{11} [b]	$E_{22} = E_{33}$ [b]	$G_{12} = G_{13}$ [b]	G_{23} [b]	$v_{12} = v_{13}$ [b]	v_{23} [b]	V_f [a]
HS	143 GPa	6.5 GPa	3.1 GPa	2.6 GPa	0.25	0.23	0.481
LS	277 GPa	4.7 GPa	2.7 GPa	2.0 GPa	0.25	0.12	0.513

Properties of the cohesive elements embedded in LS layer

$G_{Ic} = G_{IIc} = G_{IIIc}\ (N/mm)$	$\sigma_n^0 = \tau_{tn}^0 = \tau_{sn}^0 (MPa)$	$K (MPa/mm)$
1	$2217 - 2618$	10^9

Properties of the cohesive elements at the HS/LS interface

$G_{Ic}\ (N/mm)$	$G_{IIc} = G_{IIIc}\ (N/mm)$	$\sigma_n^0 = \tau_{tn}^0 = \tau_{sn}^0 (MPa)$	$K (MPa/mm)$
0.199	0.5	67	10^5

Geometric parameters

$l\ (mm)$	$b\ (mm)$	$h\ (mm)$	$h_{HS}\ (mm)$	$h_{LS}\ (mm)$
80.0	20×0.5	0.160×0.5	2×0.0323	0.5×0.0308

Finite elements mesh details

Elements number	*Elements in the length / type*	*Elements in the width*	*Elements in the HS thickness*	*Elements in the LS thickness*
230040	320 / C3D8 319 / COH	40	5	3

[a] Based on manufacturer's data [5]
[b] Calculated using manufacturer's data and Chamis model [9]

According to the literature, the range for the interlaminar shear strength is 67 - 100 MPa [4,10]. Since no data on the interlaminar shear strength was provided in [5], 67 MPa was adopted as conservative value. The fracture energy of the cohesive interface was set to 0.5 N/mm using the failure criterion proposed in [5].

As in [4], the modulus of the Weibull distribution is set to m = 41, which allows the distribution to match the experimentally observed scatter of carbon ply failure strain [10]. The characteristic strength of the LS layer for the Weibull distribution is set to 2342 MPa in order to have the first failure at 2217 MPa, which was calculated by the Hooke's law and reference data [5]. Then, the strength is randomly assigned among the cohesive elements in the range 2217 MPa - 2618 MPa (Table 1).

Table 1 also details the mesh features of the model. The specimen is discretized as follows, considering symmetries: 639 bulk elements along the length of the HS layer; 320 bulk elements and 319 cohesive elements simulating cracks in the LS layer; the LS layer has 3 elements in the thickness direction (Y), and each of the two HS layer has 5 elements with bias ratio of 10 in the thickness direction (Y); one element composes the thickness of the remaining cohesive layer, which brings the total of 9 elements along the thickness; the width has 40 elements of 0.25 mm, a typical dimension for cohesive elements [7,10].

The results of the modelling of the UD thin-ply all-carbon hybrid laminate [T_2/M/T_2] are presented in the Figure 2. The map of the stress component in the X direction in Figure 2b has been taken at a global stress level of 1400 MPa, which is almost in the middle of the pseudo-ductile plateau.

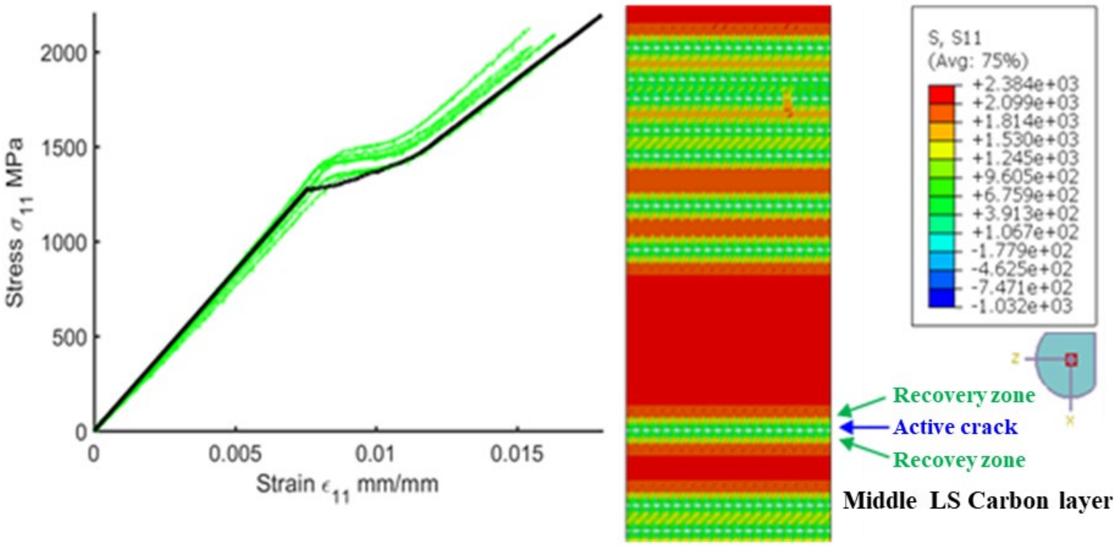

(a) (b)

Figure 2. UD thin-ply all-carbon hybrid laminate: (a) tensile stress-strain comparison, experimental data (green curves) and FE model prediction (black curve); (b) prediction of the fragmentation distribution for a global stress level of 1400 MPa.

In the elastic region, the load is mostly carried by the LS material, being stiffer than the HS material. The first ply fails at stress of 1386 MPa. Then, the plateau region starts. Activation of each new crack transfers stress from the LS layer to the HS layer via the interface. The interlaminar fracture toughness is high enough to avoid catastrophic delamination and to transfer the load to the HS layer without damage. So, the stress keeps increasing in the LS layer, leading to more fragmentation. In other words, a high interlaminar fracture toughness hinders the onset and propagation of delamination. This progressive transfer of load creates the pseudo-ductile behavior of the laminate.

According to the criterion proposed in [7], the recovery length $l_c/2$ of the laminate [T_2/M/T_2] is about 1.11 mm. Since the bulk element length is 0.25 mm, at least 8 neighbor cohesive elements (cracks) are not activated due to the low stress level. This also depends on the strength random distribution. This event is shown in Figure 2b with activated crack, recovery zone (green) and far-field stress zone (red).

The same approach was used to determine the mechanical response of different layups, varying the LS thickness ratio. The LS thickness ratio corresponds to the ratio between the LS thickness and the thickness of the laminate. According to the results in Figure 3, the laminate [T_9/M_4/T_9] and [T_2/M/T_2] have a LS thickness ratio relatively close, 17% and 19%, respectively, while the thickness of the [T_9/M_4/T_9] laminate is 4.5 times higher than the [T_2/M/T_2] laminate. The thinner laminate [T_2/M/T_2] results in pseudo-ductile behavior and the thicker laminate [T_9/M_4/T_9] in catastrophic delamination.

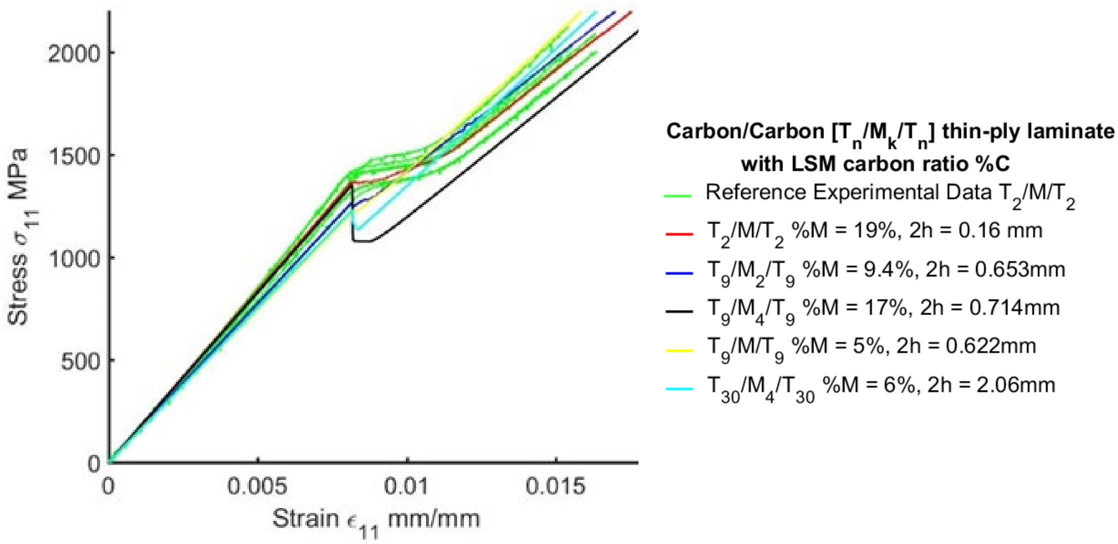

Figure 3. UD thin-ply all-carbon hybrid laminate: tensile stress-strain comparison, green curves are experimental data [T_2/M/T_2] and other colored curves are the FE model response of different layups [T_n/M_k/T_n]. The legend gives the laminate layup, the LS thickness ratio and the total thickness of the laminate.

4. Conclusions

This study was devoted to the numerical modelling of the tensile damage evolution of interlayer-hybrid laminates. The results obtained by the FE model are consistent with the experimental reference data of thin-ply all-carbon hybrid laminate [5]. The achievement of the pseudo-ductile behavior is only possible using a tough interface [5] and a sufficiently high number of embedded cohesive elements with a realistic strength distribution. The latter considerably increases the computational cost of the simulation. Convergence issues may be faced if the interface stiffness is too high and if the viscosity of the interface is too low. The selected values (Table 1) allow us to obtain a consistent numerical solution in an acceptable computational time.

Further analyses, assuming the featured of the present finite element model, will be dedicated to thick-ply all-carbon hybrid laminates and the construction of damage mode maps by modelling new layups of the interlayer hybrid laminates. The maps will help to distinguish catastrophic delamination and pseudo-ductile behavior as function of the LS thickness ratio.

Acknowledgements

The work leading to this publication was performed within the framework of HyFiSyn project and has received funding from the European Union's Horizon 2020 research and innovation programme under the Marie Skłodowska-Curie grant agreement No. 765881. Amaury Ollic acknowledges KU Leuven partial support of his research stay in Leuven and the access to the Vlaams Supercomputer Centrum.

5. References

[1] Swolfs Y, Gorbatikh L, Verpoest I. Fibre hybridisation in polymer composites: A review. Compos Part Appl Sci Manuf 2014;67:181–200. https://doi.org/10.1016/j.compositesa.2014.08.027.

[2] Dong C, Duong J, Davies IJ. Flexural properties of S-2 glass and TR30S carbon fiber-reinforced epoxy hybrid composites. Polym Compos 2012;33:773–81. https://doi.org/10.1002/pc.22206.

[3] Swolfs Y, Gorbatikh L, Verpoest I. Stress concentrations in hybrid unidirectional fibre-reinforced composites with random fibre packings. Compos Sci Technol 2013;85:10–6. https://doi.org/10.1016/j.compscitech.2013.05.013.

[4] Jalalvand M, Czél G, Wisnom MR. Numerical modelling of the damage modes in UD thin carbon/glass hybrid laminates. Compos Sci Technol 2014;94:39–47. https://doi.org/10.1016/j.compscitech.2014.01.013.

[5] Czél G, Jalalvand M, Wisnom MR, Czigány T. Design and characterisation of high performance, pseudo-ductile all-carbon/epoxy unidirectional hybrid composites. Compos Part B Eng 2017;111:348–56. https://doi.org/10.1016/j.compositesb.2016.11.049.

[6] Turon A, Dávila CG, Camanho PP, Costa J. An engineering solution for mesh size effects in the simulation of delamination using cohesive zone models. Eng Fract Mech 2007;74:1665–82. https://doi.org/10.1016/j.engfracmech.2006.08.025.

[7] Jalalvand M, Czél G, Wisnom MR. Damage analysis of pseudo-ductile thin-ply UD hybrid composites – A new analytical method. Compos Part Appl Sci Manuf 2015;69:83–93. https://doi.org/10.1016/j.compositesa.2014.11.006.

[8] Kaw AK. Mechanics of Composite Materials. 0 ed. CRC Press; 2005. https://doi.org/10.1201/9781420058291.

[9] Balzani C, Wagner W. An interface element for the simulation of delamination in unidirectional fiber-reinforced composite laminates. Eng Fract Mech 2008;75:2597–615. https://doi.org/10.1016/j.engfracmech.2007.03.013.

[10] Wisnom MR. Relationship between strength variability and size effect in unidirectional carbon fibre/epoxy. Composites 1991;22:47–52. https://doi.org/10.1016/0010-4361(91)90102-M.

